应用联合时频分析研究 CO_2 焊接过程中的电信号

罗 怡
（重庆工学院 材料科学与工程学院，重庆 400050）

摘 要：CO_2 焊接过程的电弧电压、焊接电流信号蕴含了丰富的焊接信息。利用联合时频分析对 CO_2 焊接过程电信号进行研究，分析了短时傅里叶变换窗函数的选择对谱图的时频集聚性的影响，并选择汉宁窗获得了较好的时频集聚性。为了获得 CO_2 焊接电信号中短路过渡的信息，尝试利用时频分析谱图对焊接试验中采集到的几组焊接电流信号进行分析，研究了其能量分布及熔滴过渡的特征，并利用联合时频分析三维谱图，对采用不同焊接参数获得的电弧电压信号进行对比。结果表明，利用联合时频分析对 CO_2 焊接过程电信号进行分析，能够获得更多的有价值信息，该方法具有较好的研究应用前景。

关键词：联合时频分析；CO_2 焊接；短时傅里叶变换
中图分类号：TG444 文献标识码：A 文章编号：0253－360X(2007)02－075－04

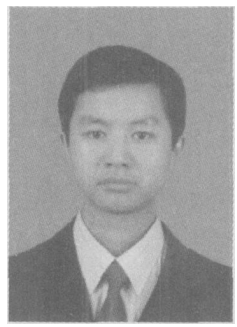

罗 怡

0 序 言

CO_2 焊接过程是一种不但受多参数制约，而且又受许多随机干扰因素影响的复杂的工艺过程。电弧物理和 CO_2 焊接过程飞溅问题的进一步研究表明，电弧燃烧情况是决定焊接质量的关键因素，而 CO_2 短路过渡焊接过程的电弧电压和焊接电流信号波动中，则蕴含了熔滴过渡飞溅和与焊接质量有关的信息。通过实时采集焊接过程中的电流、电压信号并经过一定的信号处理和相关分析，可以实现对焊接质量的监测和评估，并为全面评价焊接工艺过程，分析缺陷产生的原因提供重要的客观依据。

传统的信号分析方法是信号单独在时域或频域中进行分析。但是，信号的时域特性和频域特性并不是独立的，在分析时变为非平稳信号时，还希望进一步了解该信号在某一时刻附近的频域特性。若此时再利用傅里叶变换(FT)来分析，已不能满足局部时频域匹配检测的要求了。而联合时频分析(joint time-frequency analysis，JTFA)可以同时在时域和频域中对信号进行分析，这有助于更好地了解和处理特定的信号。

CO_2 焊接过程受各种因素的干扰，其电信号是一种频率随时间变化的非线性、非平稳信号，此时采用傅里叶变换不利于对信号做局部分析。为此，作者提出了将联合时频分析应用于弧焊过程的电信号分析，把采集到的电信号在时频空间离散化，更好地表达信号的突变特征，弥补傅里叶变换的不足。

收稿日期：2006－02－24

1 联合时频分析

联合时频分析能将一维时域信号映射到二维时频平面来观察信号的时频联合特征，构成信号的时变谱，主要用于观察信号的功率谱随时间变化的分布规律，以及信号各频率分量如何提取。对于信噪比很低的信号，无论从时域还是频域都很难将有用信号提取出来，联合时频分析则是信号检测与估计的有力工具。

1.1 不确定原理(uncertainty principle)

这里引入的不确定原理，即联合时频分析中著名的 Heisenberg 不等式，其表达公式[1]为

$$\Delta t \Delta f \geqslant \frac{1}{4\pi}, \tag{1}$$

式中：Δt 和 Δf 分别表示某函数的时间分辨率和频率分辨率。

不确定原理说明不存在既有任意小的时间长度又有任意小的频率带宽的窗函数，要获得高的频率分辨率只有以牺牲时间分辨率为代价；相反，要获得高的时间分辨率也只有以牺牲频率分辨率为代价。

也就是说，若一个函数有一个短的持续时间，它必定在频域具有宽的带宽，反之亦然。

1.2 短时傅里叶变换

短时傅里叶变换（short-time fourier transform，STFT）[2] 是目前最常用的线性时频变换，可以用快速傅里叶变换（FFT）实现，其计算速度在目前的众多时频分析方法中是最快的，而且分析结果有明确物理解释，因此在实际中得到最广泛的应用。

STFT 理论通过对信号进行预加局部化时窗来解决信号的时间－频率联合表示问题。信号 $x(\tau)$ 的连续短时傅里叶变换定义为

$$STFT_x(t,f)=\int_{-\infty}^{+\infty}x(\tau)W^*(\tau-t)e^{-j2\pi f\tau}d\tau, \quad (2)$$

式中：$W(\tau)$为一时间宽度很小的时窗。式(2)表示信号 $x(\tau)$乘上一个以 t 为分布中心的“分析时窗 $W^*(\tau-t)$”所做的傅里叶变换。由于乘以一个相当短的时窗 $W^*(\tau-t)$，等价于取出信号在分析点 $\tau=t$ 附近的一个切片，所以 $STFT_x(t,f)$可视为信号 $x(\tau)$在“分析时间”t 时刻处的“局部频谱”。

STFT 经常用到的是二次型时频表示——谱图(SPEC)，定义为 $STFT_x(t,f)$模值的平方，即

$$SPEC(t,f)=|(STFT(t,f)|^2。 \quad (3)$$

通过谱图分析能揭示信号能量在时频面上的分布情况，即时频分布。

1.3 短时傅里叶变换窗函数

将式(2)做一定变换，令

$$W^*(T)=W^*(\tau-t)e^{-j2\pi f\tau}。$$

由式(2)可得

$$STFT_x(t,f)=\int_{-\infty}^{+\infty}x(\tau)W^*(T)d\tau。(4)$$

可以看出，式中 $W^*(T)$是基函数，为一调频窗。根据不确定原理，基函数 $W^*(T)$的时频特性决定了 STFT 时频分析品质的高低。若要求 STFT 具有高的时间分辨率就要求一个较短的窗；反之，若要求 STFT 有好的频率分辨率，则需要一个较宽（相应频率带宽较窄）的时窗。

这里以 CO_2 焊接过程电弧电压信号的 STFT 谱图分析来说明分析时窗的选择对时频分析品质的影响。图 1 为一电弧电压信号，图 2a 为选择 1 024 点矩形窗情况下对图 1 电弧电压信号时频分析的结果，由于时窗相对于信号的变化而言太宽，该信号的谱图不能得到好的时频集聚性，分析结果不理想；图 2b为选择 256 点矩形窗情况下的分析结果，在此情况下，谱图的时频集聚性得到一定的改善；图 2c 为选择 256 点汉宁窗（hanning）情况下的分析结果，相对于以上情况，谱图的时频集聚性最好，可以得到较理想的分析结果。因此，后续部分的时频分析均选择汉宁窗来完成。

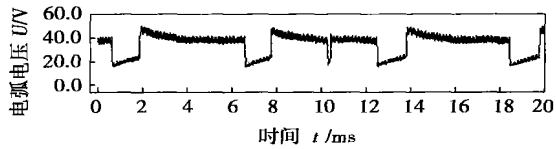

图 1 电弧电压信号

Fig. 1 Signal of arc voltage

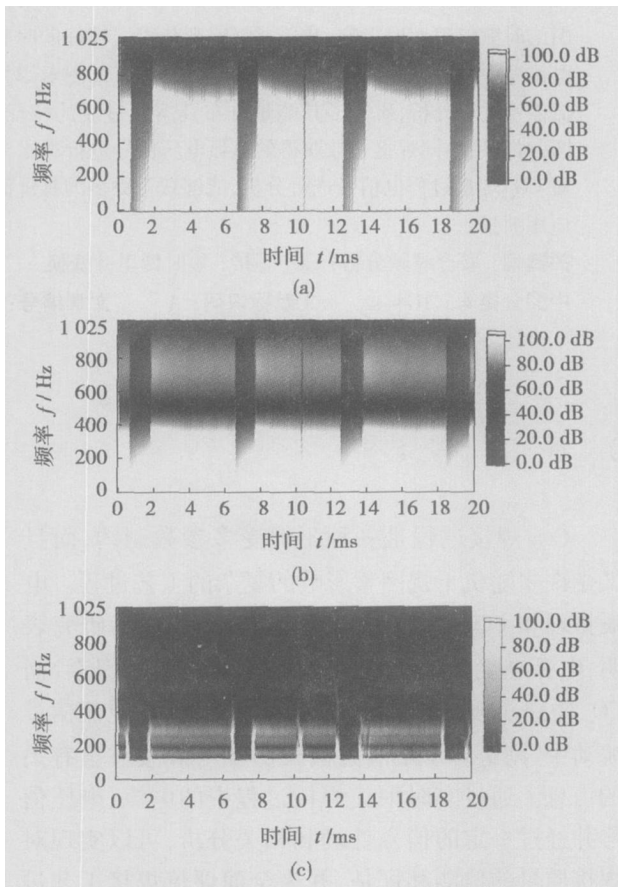

图 2 分析窗选择对时频分析谱图影响

Fig. 2 Effect of analysis window on result of spectrum of time-frequency analysis

2 CO_2 焊接过程检测系统

试验检测系统由霍尔传感器、基于 C8051F320 单片机开发的数据采集器、工控机等部分组成。数据采集频率设为 5 kHz，通过高速 A/D 转换将采集到的电弧电压和焊接电流信号通过 USB 总线高速传输到工控机，由分析软件系统处理得出结果。试验中使用的焊接电源为德国产 Phoenix 300 全数字化多功能电焊机；选用焊丝 H08Mn2SiA，焊丝直径 ϕ1.2 mm；保护气体 100%CO_2，气体流量 15 L/min；母材为 Q235B，

板厚 6 mm。

3　试验结果及分析讨论

试验过程在母材上堆焊，并采用正交法设计试验方案。电弧电压选用 18，20，22 V 三个参数；焊接电流选用 150，160，170 A 三个参数；焊接速度选用 35，45，55 cm/min 三个参数进行正交试验，试验方案及试验现象如表 1 所示。

表 1　CO_2 焊接正交试验方案及结果

Table 1　Schemes and results of orthogonal test of CO_2 arc welding

试验编号	电弧电压 U/V	焊接电流 I/A	焊接速度 v/(cm·min^{-1})	试验现象
1	18	150	35	焊接不稳定，飞溅小，成形较好
2	20	150	45	焊接较稳定，飞溅小，成形较好
3	22	150	55	焊接不稳定，飞溅较大，成形差
4	18	160	45	焊接很不稳定，飞溅大，成形很差
5	20	160	55	焊接较稳定，飞溅小，成形较好
6	22	160	35	焊接较稳定，飞溅小，成形较好
7	18	170	55	焊接很不稳定，飞溅大，成形很差
8	20	170	35	焊接较稳定，飞溅小，成形较好
9	22	170	45	焊接稳定，飞溅很小，成形好

有研究认为[3]，CO_2 焊的成形问题受焊丝直径、焊接电流、电弧电压、焊接速度、焊件厚度及焊接位置等的影响，但主要决定于熔滴过渡特点。CO_2 焊接过程以短路过渡为主，短路过程中，短路与燃弧交替进行，使电阻热与电弧热能量向焊丝和焊件分配。当燃弧期间与短路期间的能量比很大时，焊缝成形平坦、光滑、熔深较大；反之，焊缝成形窄而高。可见，对 CO_2 焊接过程能量分布在时域上的变化规律的识别可作为研究 CO_2 焊接焊缝成形的要素之一。

图 3 是试验 2 和试验 5 两组短路期和燃弧期的时间规律分配不同的相似焊接电流信号，即两个在不同时刻以不同方式变化但含有相似频率成分的非平稳信号。由于傅里叶变换只适用于做全局分析，因此，从图 3a，b 的傅里叶频谱分析图可以看到，两个信号的频谱几乎完全相同，无法揭示两个信号中频率成分随时间的变化规律。然而，图 3a，b 的时频谱图则清晰地显示了这两个信号频率的发生时间和变化规律的截然不同。即谱图表明，两个信号在时频平面上的能量分布是完全不同的，使用联合时频分析可以区分这两个信号。

图 4 是取自试验 3 的一组焊接电流信号。该组试验焊接过程中包含有瞬时短路和焊接电流过大等

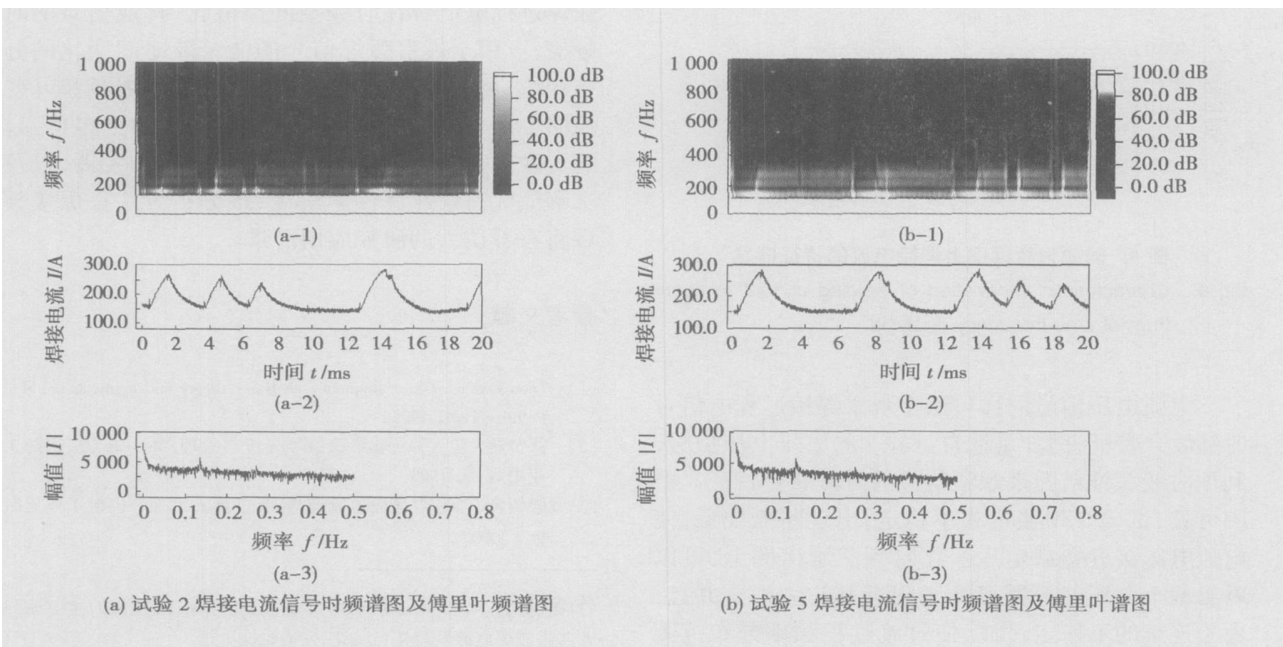

图 3　两个具有相似傅里叶频谱的不同焊接电流信号

Fig 3　Two different welding current but corresponding to same Fourier spectrum

情况。从谱图中可以看出，该组信号能量主要分布在频率 100 Hz 左右。焊接电流曲线发生突变处，也就是短路过渡颈缩开始发生的时刻以及电弧开始燃烧的时刻，在时频分析谱图上都会对应着明显的频

率变化，突变幅度越大，频率变化越强烈。这包含着在短路与燃弧交替进行过程中，频率及焊接能量变化的规律。提取出这些特征信息，也可以准确地判断出短路过渡颈缩发生时刻及燃弧开始时刻。另外，在时域波形图上还可看出，前三个焊接电流波形不规则，这表明焊接过程并不稳定。从时频分析谱图上分析，第一个焊接电流波形，出现一次瞬时短路，该瞬时短路产生频率扰动在 160 ~ 360 Hz 内。随后的燃弧过程经历了较长时间，有足够时间形成较大的熔滴，使紧接着的短路过渡形成较大飞溅，造成连续的焊接电流过大，并含有瞬时短路，焊接过程不稳定，使焊缝成形较差。这一不稳定过程的频率扰动较第一个焊接电流波形更强烈，范围分布在 160 ~ 500 Hz 之间。之后焊接过程逐渐趋于平稳。从时频分析谱图上提取这一焊接过程中不稳定的频率及能量因素，便可以准确判断能量分布对焊缝成形的影响。

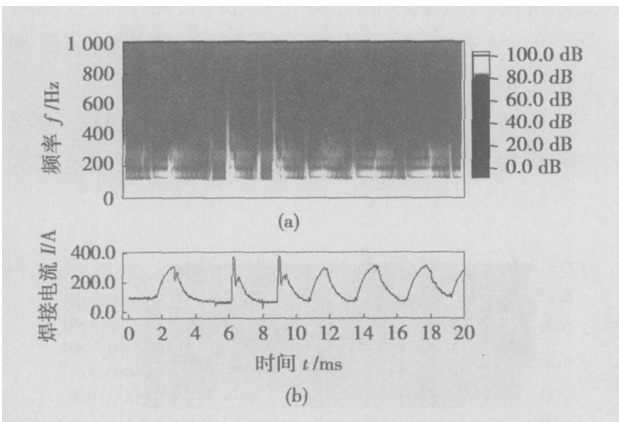

图 4 时频分析谱图上焊接电流的特征信息

Fig. 4 Characteristic information of welding current in spectrum of time-frequency analysis

电弧电压信号同样可用于观察焊接过程电信号时频联合特征，图 5 是取自试验 7 的电弧电压信号，利用时频三维谱图来观察信号的时频联合特征。由图可见，试验 7 焊接过程不稳定，出现断弧现象，使电弧电压接近空载电压。在时频三维谱图上，可以看出两个电压波形明显高于附近其它波形。并且，由于连续的不稳定过渡，使过渡过程频率分布范围较宽，从频域上可以看到，直至1 000 Hz 都有能量分布，在断弧出现的时域对应的频率变化强度更大，分布在 800 Hz 左右。

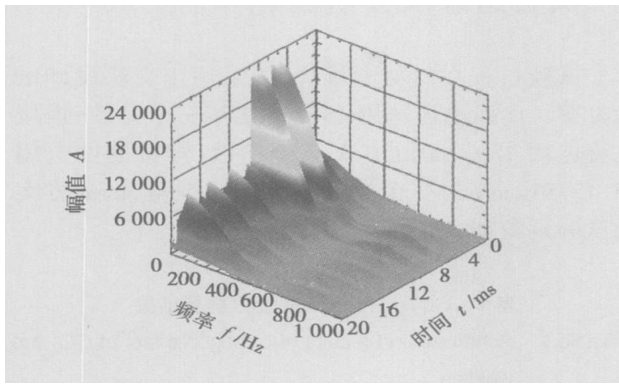

图 5 时频分析三维谱图上的电弧电压特征信息

Fig. 5 Characteristic information of arc voltage in 3D spectrum of time-frequency analysis

4 结 论

研究以 STFT 线性时频变换为基础，并选择合适的时窗，可以使时频谱图获得好的时频集聚性。由试验可以证明，应用联合时频分析可以把采集到的弧焊过程电信号在时频空间离散化，构成信号的时频谱，可用于观察弧焊信号的能量随时间变化的分布规律，更好地表达信号的突变特征，弥补傅里叶变换的不足，从而揭示焊接过程中信号的更多信息。随着联合时频分析理论的进一步研究和发展，以及求解最优窗快速算法的解决，该分析方法在焊接领域将有着诱人的研究应用前景。

参考文献：

[1] Leon Cohen. Time-frequency analysis: theory and applications[M]. Prentice Hall, 1995.

[2] 张贤达，包 铮. 非平稳信号分析与处理[M]. 北京：国防工业出版社，1998.

[3] 殷树言. CO_2 焊接设备原理与调试[M]. 北京：机械工业出版社，2000.

作者简介：罗 怡，男，1979 年出生，工学硕士，助教。主要研究方向为弧焊电源及焊接自动化，发表论文 5 篇。

Email：luoyi@cqit.edu.cn

9.5% more than Fe—Cr—C hardfacing alloy. And the relative abrasion wear-resisting property of NbC strengthened Fe—Cr—C hardfacing alloy increased 60% comparing to the Fe—Cr—C hardfacing alloy. The cross shape of NbC hard phase in Fe—Cr—C—NbC alloy is erose, showing as rhombic or polygonal shape distributed between the M_7C_3 or embed in the M_7C_3. The distribution of NbC phase is not uniform, and it congregates in local regions. The eutectic carbides in the Fe—Cr—C—NbC alloy show coarse structure compared to the Fe—Cr—C hardfacing alloy, and the space betweer them is much great.

Key words: Fe—Cr—C hardfacing alloy; NbC; abrasion wear-resisting property; microstructure

Ductile tearing assessment of surface flaw in circumferential weld of pipe-line based on *J* integral parameter ZHANG Manli[1], WANG Jianping[2], TAO Yongyin[2] (1. Maths and Information Department, Langfang Teachers College, Langfang 065000, Hebei, China; 2. Research Institute of China Petroleum Pipeline Bureau, Langfang 065000, Hebei, China). p59—62, 66

Abstract: Based on level three programme (ductile tearing assessment) of assessment standard BS7910, ductile tearing assessment of surface flaw in circumferential weld of pipe-line under pure bending load was proceeded by using J integral engineering estimate method of SC. ENG. By taking X56 steel pipeline as an example, effects on assessment curve and evaluating results were given by flaw dimension and fracture parameter choosing were discussed, and the assessment point was put forward that J_{mat} is more reasonable than J_g in determining assessment points while choosing J integral parameter to make a ductile tearing assessment of flaw in metal structure. The research results are not only taken as a guide on safty evaluation in pipeline construction, but also can make engineering application of the ductile tearing assessment of structure with flaw more popular and referentia.

Key words: BS7910; J integral; circumferential weld; surface flaw; ductile tearing assessment

Characteristic of interface microstructure in joint between copper alloy and 35CrMnSiA steel LV Shixiong, YANG Shiqin, WANG Haitiao, XUE Chengbo (State Key Laboratory of Advanced Welding Production Technology, Harbin Institute of Technology, Harbin 150001, China). p63—66

Abstract: The shell structure consisting of copper alloy surfacing layer and steel substrate was produced by a cool-body tungsten inert gas surfacing method, and microstructure of the shell was mainly investigated. Characteristics of microstructure and morphology of interface, copper alloy layer and steel substrate were observed by using optical microscope, scanning electron microscope. Effects of welding process on the content of Fe within the copper alloy were also analyzed. Energy dispersive X-ray analysis on the composition change of coppr alloy layer and interface shows that solution of some elements from the steel substrate to the copper alloy layer and diffusion of some elements of copper alloy layer to the steel substrate happened during the welding process. There is Fe_2Si distributing in the copper alloy layer dispersely when CuSi3 is used as surfacing layer and there is dendritic crystal in the copper alloy layer when surfacing layer is made of B30. Moreover, penetration cracks caused by eutectoid at the interface occurred when the inappropriate welding parameters were used.

Key words: coppe alloy; steel; tunsten inert-gas surfacing; interface

Gas in weld for self shielded flux-cored arc welding YU Ping[1], TIAN Zhiling[1], PAN Chuan[1], XUE Zhenkui[2] (1. National Engineering Research Center of Advanced Steel Technlogy, Centeral Iron & Steel Research Institute, Beijing 100081, China; 2. Research Institute of China Petroleum Pipeline Bureau, Langfang 065000, Hebei, China). p67—70, 74

Abstrat: The nitrogen content in the weld for FACW—S (flux cored arc welding-self-shielded) is about 0.025%—0.035%, which is higher than other welding materials. The effects of flux ingredients(for example: fluoride, carbonate and nitrogen fixation substance Al) on the nitrogen gas pore were studied. The welding parameters also have an important influence on the nitrogen gas pore. Considering the gas pore in the weld, the welding parameters should be 220—280 A welding current, 18—24 V welding voltage, 20—30 mm wire extension and direct current stright polarity. Hydrogen gas pore and CO/CO_2 gas pore are not easy to form in FCAW—S weld.

Key words: self-shielded flux-cored wire; nitrogen porosity; influencing factors

Influence of local heating-cooling on welding residual stress of francis turbine runner JI Shude[1], ZHANG Liguo[1], FANG Hongyuan[2], LIU Xue-song[2] (1. Institute of Astronautical Technology, Shenyang Institute of Aeronautical Engineering, Shenyang 110034, China; 2. State Key Laboratory of Advanced Welding Production Technology, Harbin Institute of Technology, Harbin 150001, China). p71—74

Abstrat: On basis of local heating-cooling method which is brought out to improve the distribution of welding residual stress in blade according to the property of weld formation, influence of local heating-cooling method on runner's residual stress field is studied by numerical simulation technology. Moreover, the change process of welding stress in the blade dangerous area and the optimizing scheme of local heating are attained. The result shows that the method of local heating-cooling can decrease the residual tensile stress peak in dangerous area of the blade. The effect on decreasing residual stress is directly proportional to heating time, heating temperature and heating area. Moreover, with the augmentation of heating distance, the residual stress in dangerous area can decrease and with further the augmontation the residual stress will increase.

Key words: blade; local heating-cooling; numerical simulation; welding residual stress

Application of joint time-frequency analysis to electrical signals of CO_2 arc welding LUO Yi (School of Material Science and Engineering, Chongqing Institute of Technology, Chongqing 400050, China). p75—78

Abstract: The electrical signals of CO_2 arc welding contain plenty of welding information. The joint time-frequency analysis was used to study the electrical signals of CO_2 arc welding. The effect of analysis window selecting of short-time Fourier transform to the result of time-frequency analysis spectrum was discussed, and the conclusion that Hanning window has better time-frequency centralizing in analysis was gotten. Based on several welding currents and arc voltages in experiment, the characteristic of energy distribution and metal transfer was investigated by time-frequency analysis to get the information of short-circuiting transfer in electrical signals of CO_2 arc welding. The result of analysis in experiment shows that more information in electrical signals can be gotten by time-frequency analysis in CO_2 arc welding. This way has a good foreground in research and application.

Key words: joint time-frequency analysis; CO_2 arc welding; short-time Fourier transform

Effect of thermit composition on manual SHS welding for low carbon steel LI Zhizun, XIN Wentong, WU Bin, LI Baofeng (Advanced Material Institute, Ordnance Engineering College, Shijiazhuang 050003, China). p79—81

Abstract: Base on self-propagating high-temperature synthesis(SHS), a new method of welding called manual SHS welding is introduced. Since it is easy to carry and operate, this technique can be used in emergency maintenance. The effect of the thermit composition of the combustion welding rod on the welding of low carbon steel and the microstructure of weld were studied. The thermit was composed of (CuO+Al) and (Fe_2O_3+Al). It is shown that when the content of (CuO+Al) is higher than 50%, welding can successfully proceed. And combustion velocity becomes higher with the increasing of (CuO+Al) content. This is due to the higher combustion temperature and larger combustion heat of (CuO+Al) thermit. The tensile strength of weld becomes higher with the increasing of (Fe_2O_3+Al) content. This is due to the precipitation of the second phase rich in Fe, which can thin the Cu grain and strengthen the alloy. The combustion welding rod with 50% and 60% (CuO+Al) thermit is easy to operate and the tensile strength of weld are higher than 420 MPa.

Key words: manual self-propagating high-temperature synthesis welding; thermit; combustion velocity; tensile strength

Microstructure and residual stress of TA12 titanium alloy with electron beam welding FU Pengfei[1], HUANG Rui[2], LIU Fangjun[1], ZUO Congjin[1](1. Key Laboratory of High Energy Density Beam Processing Technology, Beijing Aeronautical Manufacturing Technology Research Institute, Beijing 100024, China; 2. Qian Han Pipe Factory, Chengdu Aircraft Industrial Group Co., Ltd., Chengdu, 610092, China). p82—84

Abstract: Weld configuration of TA12 titanium alloy is very good for electron beam welding(EBW). The main microstructure of weld is martensite, and the tiny rare earth rich phases is dispersedly distributed in the weld zone, and dimension whose configuration changes disciplinary along the joint. By hole drilling method measuring weld residual stresses, the results show that longitudinal stresses are higher than transverse stress, which present gradient distribution along the vertical direction of the weld. In the weld all the longitudinal residual stresses are tensile stresses, and whose peak stresses are lower than yield stresses, while the transverse stresses are very low pressure stresses. Along the weld direction in the central of the plate the residual stresses distributing are approximate equal.

Key words: TA12 titanium alloy; electron beam welding; rare earth phase; residual stress

Effects of shielding gas in CO_2 laser—MAG hybrid welding GAO Ming, ZENG Xiaoyan, HU Qianwu, YAN Jun (School of Optoelectronics Science and Engineering, Huazhong University of Science and Technology, Wuhan 430074, China). p85—88

Abstract: Shielding gas is acrucial factor for the process stability, weld penetration and joint quality of CO_2 laser—MAG (mental active gas) hybrid welding. However, the concerned researches about this field are very few. A serial trial investigating the effect of He—Ar and CO_2—Ar shielding gas on CO_2 laser—MAG hybrid welding was carried out on mild steel. The results show that different mixed shielding gases have different effects. The penetration depth and microhardness of He—Ar welds are hisher than that of CO_2—Ar welds. Because atomic oxygen is decomposed from CO_2 under high temperature and enters into welding pool, the surface tension coefficient changes and the direction of weld pool flow is changed. Consequently, CO_2—Ar weld reinforcement becomes flatter at $CO_2 \geqslant 30\%$ and the transition from arc zone to laser zone is flatter. Moreover, when $CO_2 > 30\%$, the process stability and microhardness of weld dramatically decrease.

Key words: laser welding; arc welding; hybrid welding; shielding gas; welding penetration

A CO_2 arc welding seam detection algorithm based on transition region YANG Fugang, SUN Tongjing, ZHANG Guangxian, PANG Qingle (School of Control Science and Engineering, Shandong University, Jinan 250061, China). p89—91

Abstract: In order to detect CO_2 arc welding seam, a new image segmentation method based on transition region is presented. Transition region is a special region located between the object and background in the real image, whose histogram has a wide and evenly hollow between two peaks. First, transition region of original image is determined by calculating the average grads of nonzero pixels of the image obtained through top-cut and bottom-cut transform, and then threshold can be obtained easily from transition region. It overcomes the effect of disturbance. Examinations indicate that it is a good method to detect CO_2 arc welding seam.

Key words: CO_2 arc welding; edge detection; seam detection; transition region

Application of vibratory welding technology to large-scale welding components LU Qinghua, CHEN Ligong, NI Chunzhen, RAO Delin (School of Materials Science and Engineering, Shanghai Jiaotong University, Shanghai 200030, China). p92—94, 98

Abstrat: The vibratory conditioning process was investigated